

# Sintering Ability of BaTiO<sub>3</sub> Powders Elaborated by Citric Process

C. Le Calvé-Proust,<sup>a,b</sup> E. Husson,<sup>a,b</sup> P. Odier<sup>a</sup> & J. P. Coutures<sup>a</sup>

<sup>a</sup>Centre de Recherche sur la Physique des Hautes Températures–CNRS, 1d Av. de la Recherche Scientifique, 45071 Orléans Cedex 2, France

<sup>b</sup>Laboratoire de Physique et Mécanique des Matériaux, ESEM, R. Léonard de Vinci, B.P. 6747, 45067 Orléans Cedex 2, France

(Received 7 December 1992; revised version received 24 February 1992; accepted 15 March 1993)

## Abstract

BaTiO<sub>3</sub> powders have been elaborated by several methods using mixed citrate as precursor. This compound has been used alone or dissolved in aqueous or organic solutions, giving rise to different powder morphologies (blocks of aggregates, hollow spheres, plate-like agglomerates, porous plates, blocks). The pore size distributions of the green compacted samples were measured by mercury intrusion and the sintering was followed by dilatometry. The sintering ability of these powders depends essentially on their agglomeration state determined by their elaboration mode. A powder densification mechanism is proposed.

BaTiO<sub>3</sub>-Pulver wurde mit Hilfe verschiedener Methoden aus einer Zitrat-Mischung als 'precursor' hergestellt. Der 'precursor' wurde einzeln oder in einer wässrigen oder organischen Lösung verwendet. Dies führte zu verschiedenen Pulvermorphologien (blockförmigen Anhäufungen, Hohlkugeln, plattenartigen Agglomeraten, porösen Platten, Blöcken). Die Verteilung der Porengröße in den Grünlingen wurde mit Hilfe der Quecksilberintrusion bestimmt, und nach dem Sintern wurden die Proben dilatometrisch vermessen. Die Sinterfähigkeit der Pulver hängt entscheidend von ihrem Agglomerationszustand ab, der durch die Herstellungsmethode bestimmt wird. Ein Pulververdichtungsmechanismus wird vorgeschlagen.

Les poudres de titanate de baryum ont été élaborées, à partir d'un citrate mixte, par plusieurs voies. Ce précurseur a été utilisé soit seul soit mis en solution organique ou aqueuse conduisant à des poudres de différentes morphologies (amas d'aggrégats, plaquettes, plaques poreuses, blocs). La distribution de la taille des pores a été étudiée par porosimétrie au mercure, et le frittage a pu être suivi par dilatométrie.

*L'aptitude au frittage de ces poudres dépend essentiellement de leur état d'agglomération déterminé par leur mode d'élaboration et un mécanisme de densification est proposé.*

## 1 Introduction

It is well known that the physical properties of electroceramics are sensitive to their microstructure, so control of such is essential during ceramic processing. The present authors are particularly interested in organic processes and more precisely in citric precursor methods of barium titanate preparation. BaTiO<sub>3</sub> powders have been elaborated by three methods, detailed previously,<sup>1</sup> using a Ba–Ti mixed citrate:

- Thermal decomposition of a Ba–Ti mixed citrate;
- spray pyrolysis of an aqueous solution of the same compound;
- thermal decomposition of an organic citric resin produced from this mixed citrate.

These three methods provide a way to elaborate fine BaTiO<sub>3</sub> powders. Their aggregation characteristics ('strongly bonded agglomerates') may be different but in all cases they are made of aggregates of 150 nm size. These powders are then suitable for the investigation of the effect of aggregation on sintering.

## 2 Previous Results in Powder Elaboration

### 2.1 Mixed citrate

The synthesis of the BaTi(C<sub>6</sub>H<sub>6</sub>O<sub>7</sub>)<sub>3</sub>·6H<sub>2</sub>O mixed citrate (MC) was described by Hutchins *et al.*<sup>2</sup> and

Hennings & Mayr.<sup>3</sup> In this mixed citrate, the ratio Ba/Ti = 1 is fixed and after calcination at 700°C, a pure BaTiO<sub>3</sub> powder, constituted of blocks of aggregates of 150 nm size, is obtained.

## 2.2 Spray pyrolysis of an aqueous mixed citrate solution

It is possible to dissolve the mixed citrate in an ammoniacal aqueous solution at pH = 6.3. This solution is sprayed by a piezoelectric transducer and pyrolysed in air with an appropriate furnace.<sup>1</sup> The concentration of the solution must be low ( $C = 2.3 \times 10^{-2}$  mol/litre). Annealing at 700°C gives a pure BaTiO<sub>3</sub> powder. The particles are 1 μm hollow spheres which are constituted of aggregates of 150 nm.<sup>4-7</sup>

## 2.3 Citric resin

The existence of three acidic functional groups in the mixed citrate (MC) makes it soluble in citric acid (CA)-ethylene glycol (EG)-water mixture. The resulting solutions are clear and stable with time. These solutions are polymerized at 150°C to form a mixed organic-inorganic resin which contains Ba and Ti cations.

The authors have studied, at room temperature, the isomolar cross-section of the CA-EG-H<sub>2</sub>O-1 mol MC quaternary diagram.<sup>1</sup> A mass yield expressed by:  $R = [\text{weight of BaTiO}_3]/[\text{weight of initial solution}]$  was defined. Compositions shown in zones 2 and 3 provide very viscous and white liquids or even wax. Only the compositions lying in zone 1, limited by lines 1-2-3 on Fig. 1, can give clear and stable solutions.

Powders were prepared from these clear solutions. The mixtures were calcinated at 700°C in static air and gives pure BaTiO<sub>3</sub> after 2 h. The microstructure studied by SEM shows powders constituted with

aggregates of 150 nm. Three types of morphologies have been distinguished according to the  $R$  value. If  $R$  is lower than 2, 10-μm thick plate-like agglomerates are observed, in which the 150 nm spheroid particles are regularly distributed. When  $R$  increases up to 8%, porous plates of 20 μm thickness are formed. For  $R$  ranging between 8 and 14.5%, blocks of 0.3 mm long are obtained. For  $R > 14.5\%$ , the limit of the MC solubilization in CA-EG-H<sub>2</sub>O solutions is reached.

## 3 Experimental

The powders obtained at 700°C were isostatically pressed at 250 MPa.

Sintering measurements were made in a vertical dilatometer (Setaram, Lyon, France) with a constant force load equivalent to 1 g. Experiments were conducted at a constant rate of 150°C/h. The derivative curve of shrinkage versus  $T$  may be calculated electronically and plotted simultaneously with the shrinkage after the experiment. The measurement of the shrinkage, reported for room temperature, allows estimation of the green density from the final density.

Green compacted samples and final bulk densities were measured by Archimedes' method and confirmed with mercury intrusion (Micrometric 9300, Paris, France) data. This last technique gives important information on the pore size distribution.

The purity of the powders was studied by X-ray diffraction: no extra line was observed on the X-ray patterns. No organic compound was revealed on infrared spectra. Other impurities were not detected by electronic microprobe or by the RBS method (Rutherford back scattering).

## 4 Results and Discussion

The sintering behaviour of powders obtained with the three elaboration processes is shown in Fig. 2. In all cases, the derivative of the shrinkage rate versus temperature shows a maximum at 1060°C independent of the elaboration route. This phenomenon could correspond to the elimination of porosity due to the packing of the 150 nm aggregates, because these aggregates exist in all the powders. A second maximum can be observed at a higher temperature, depending on the mode of elaboration.

For better comprehension the sintering behaviour of the powders elaborated by citric resins is reported first, then the results obtained with powders elaborated by spray pyrolysis and mixed citrate decomposition are reported.

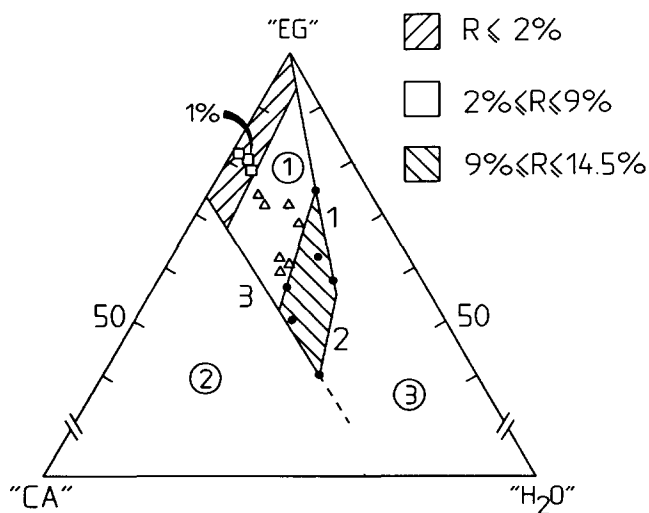


Fig. 1. Isomolar cross-section of CA-EG-H<sub>2</sub>O-1 mol MC quaternary diagram.

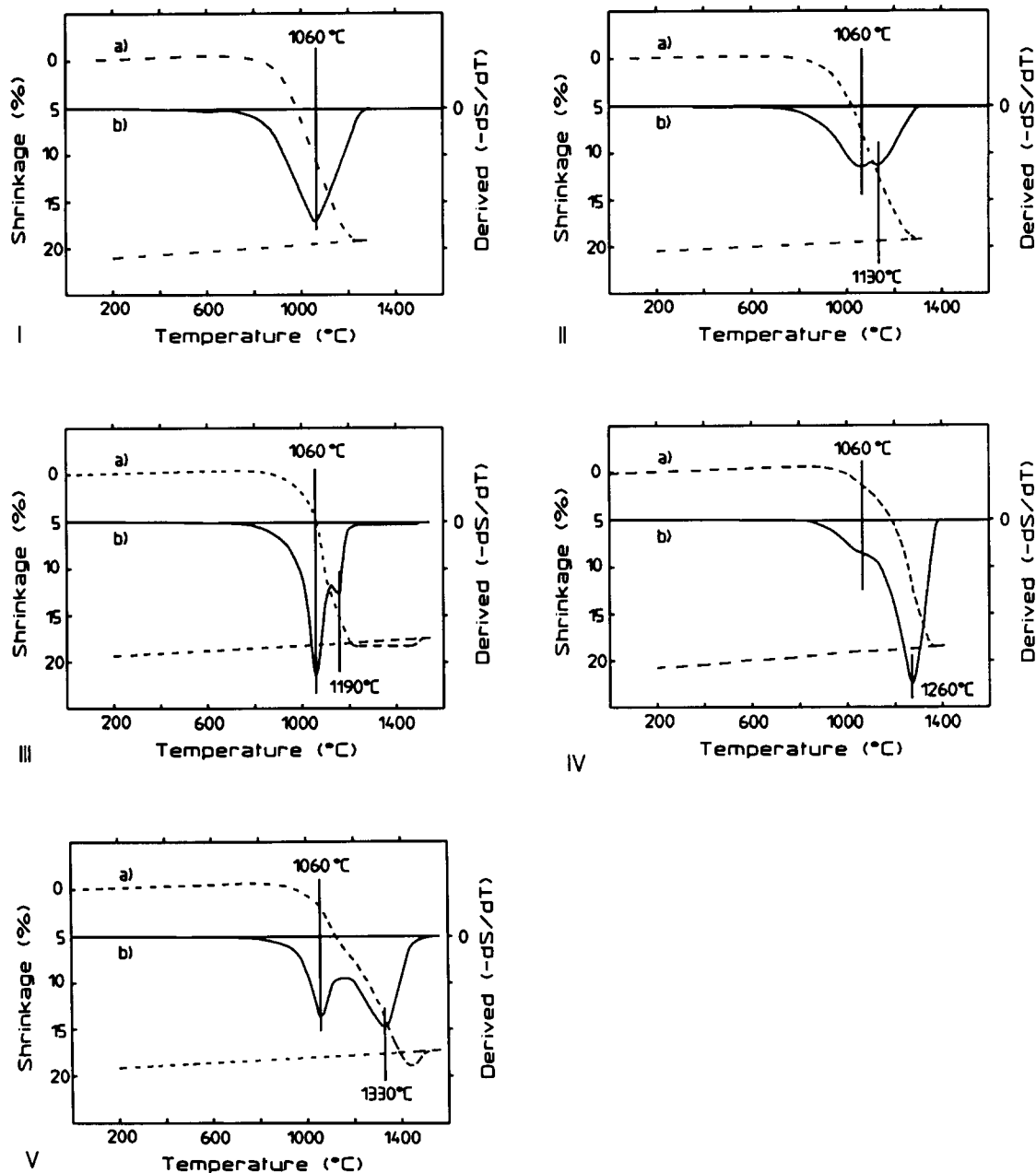


Fig. 2. Sintering of: I, deagglomerated powder from citric resin,  $R=1\%$ ; II, green powder produced from citric resin,  $R=1\%$ ; III, powder from citric resin,  $R=9\%$ ; IV, powder obtained by spray pyrolysis; V, powder from mixed citrate thermal decomposition. For each curve (a) (---) represents the shrinkage  $S$  versus  $T$  and (b) (—) the derivative over  $T$  of the shrinkage (right-hand scale).

#### 4.1 Powders elaborated by citric resins

##### 4.1.1 With deagglomeration step

The powders obtained by the citric resin process for a yield  $R=1\%$  have a high sinterability after a suitable deagglomeration step which can be accomplished by ultrasonic dispersion. The sintering ends at about  $1250^{\circ}\text{C}$  with a density approaching 99% of the theoretical density (Fig. 2(I)).

##### 4.1.2 Without deagglomeration step

Figure 2(II) shows the sintering ability of a powder ( $R=1\%$ ) obtained by the same chemical route but without deagglomeration. The sintering process slows down and ends at about  $1310^{\circ}\text{C}$  and a second maximum appears on the derivative of the shrinkage rate versus temperature. These experiments confirm

for powders elaborated by the same process the great importance of the deagglomeration step.

Similar experiments can be performed on non-deagglomerated powders with mass yields higher than 1%, as for example with  $R=9\%$  (Fig. 2(III)). The second maximum is observed to shift toward the higher temperatures. The position of this maximum depends on the mass yield. The higher the yield, the higher the temperature and the longer the time of densification. Moreover, the shrinkage curve (Fig. 2(III)) shows, at high temperature (above  $1400^{\circ}\text{C}$ ), a dedensification behaviour which could be due to gas detrapping. For the sample with  $R>9\%$ , the phenomenon is still more important.

It is possible to relate these observations with the morphology of the non-deagglomerated powder.

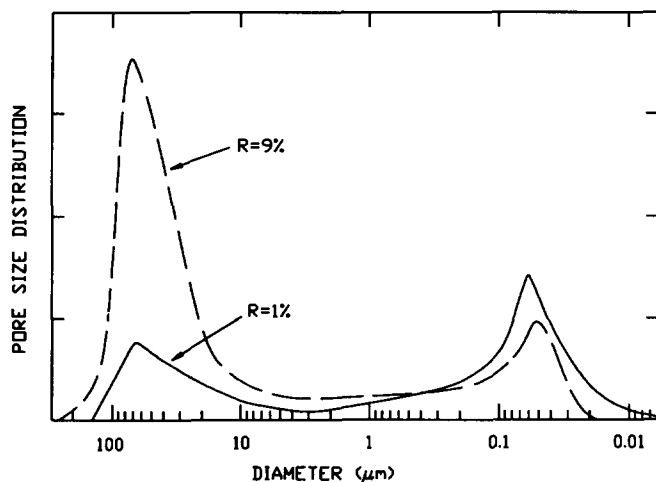


Fig. 3. Pores size distribution versus diameter of  $\text{BaTiO}_3$  (—)  $R=1\%$  and (---)  $R=9\%$  compacted sample.

The results obtained by mercury intrusion gives essentially two pore size distributions, one centred on  $0.05 \mu\text{m}$ , the other on  $80 \mu\text{m}$  (Fig. 3).

—After compacting, the green samples obtained for  $R=1\%$  and  $R=9\%$  exhibit two pore distributions, centred on pore sizes of  $0.05 \mu\text{m}$  and  $80 \mu\text{m}$  (Fig. 3).

—The volume of smallest pores ( $0.05 \mu\text{m}$ ) is practically the same in both cases. On the other hand, the number of the largest pores ( $80 \mu\text{m}$ ) is four times more important in a  $R=9\%$  sample than in a  $R=1\%$  one. Thus, the existence of a great quantity of large pores requires a higher sintering temperature in order for dense materials to be obtained.

#### 4.2 Spray pyrolysis

This method allows the production of spherical hollow-shaped powders with  $150 \text{ nm}$  aggregates. After sintering the final density approaches  $99\%$  of the theoretical density.

On the derivative of the shrinkage versus temperature, the maximum is observed at  $1300^\circ\text{C}$  with a shoulder at  $1060^\circ\text{C}$ . The shoulder could be due to the sintering of the  $150 \text{ nm}$  aggregates as in the previous cases (Fig. 2(I) and (II)) and the maximum corresponds to the elimination of the voids of the hollow spheres. It is possible to eliminate this maximum on the sintering curve at  $1300^\circ\text{C}$ , by an appropriate deagglomeration treatment, but the spheres are destroyed. This emphasizes once more the role played by the packing on the sintering process.<sup>8</sup>

#### 4.3 Mixed citrate decomposition

The powders obtained by mixed citrate decomposition were not deagglomerated before isostatic pressing. Their sintering behaviour is shown in Fig. 2(V). The first maximum of the derivative shrinkage versus temperature is observed at  $1060^\circ\text{C}$  and corresponds to the sintering of the  $150 \text{ nm}$  aggre-

gates. The temperature of the second maximum is shifted to higher temperatures (above  $1350^\circ\text{C}$ ). The densification step ends at about  $1400^\circ\text{C}$ . Beyond this temperature, a phenomenon of dedensification is observed. The  $150 \text{ nm}$  aggregates cohesion can be destroyed after a strong grinding. Under these conditions, the sintering ability is comparable with that obtained with a deagglomerated powder elaborated by the citric resin method.

### 5 Conclusion

The mixed citrate is an interesting way to prepare stoichiometric barium titanate powders. In the three methods used, the green densities and final bulk densities are respectively about  $45\%$  and  $99\%$  of the theoretical density.

The presence of the  $150 \text{ nm}$  aggregate size is independent of the elaboration method but depends on the mixed citrate itself. The influence of the nature of the precursors on the size of the final powder was pointed out by Reh Springer.<sup>9</sup> In all cases, the green densities comprise of between  $45$  and  $50\%$  of the theoretical density and after sintering reach  $99\%$  of the theoretical density.

The mass yield of the citric resin governs the powder morphology. The best sintering ability is obtained when powders are deagglomerated and the  $150 \text{ nm}$  aggregates destroyed. Thus, after isostatic pressing, samples have only one pore size distribution which is related to the  $150 \text{ nm}$  aggregates.

When the powders are non-deagglomerated, the sintering curve shows a second maximum. The presence and the shift of the second maximum is connected to the larger pore size distribution and to the agglomeration state of powders. This phenomenon has been observed during  $\text{ZrO}_2\text{-Y}_2\text{O}_3$  ( $3.2\%$ ) sintering.<sup>10</sup> The powder densification mechanism can be described by:

- Elimination of the smallest size pores or densification of the  $150 \text{ nm}$  aggregates;
- elimination of the biggest pores induced by the type of elaboration process.

Among the three elaboration processes, only the one using a citric resin leads to the best sintering ability because the corresponding powders may be easily deagglomerated.

#### Acknowledgements

This work was supported financially by the Regional Council 'Region Centre' and CNRS. The authors thank P. Canale and D. Ruffier for technical assistance.

**References**

1. Coutures, J. P., Odier, P. & Proust, C., Barium titanate formation by organic resins formed with mixed citrate. *J. Mater. Sci.*, **27** (1992) 1849–56.
2. Hutchins, G. A., Maher, G. H. & Ross, S. D., Control of Ba:Ti ratio of BaTiO<sub>3</sub> at a value of exactly 1 via conversion to BaO.TiO<sub>2</sub>.3C<sub>6</sub>H<sub>6</sub>O<sub>7</sub>.3H<sub>2</sub>O. *Am. Ceram. Bull.*, **66** (1987) 681–4.
3. Hennings, D. & Mayr, W., Thermal decomposition of (BaTi) citrates into barium titanate. *J. Solid State Chem.*, **26** (1976) 329–38.
4. Dubois, B., Ruffier, D. & Odier, P., Preparation of fine spherical yttria-stabilized zirconia by the spray-pyrolysis method. *J. Am. Ceram. Soc.*, **72** (1989) 713–15.
5. Odier, P., Dubois, B., Clinard, C., Stroumbos, H. & Monod, P., In *Ceramic Powders Science III, Ceramics Transaction*, Vol. 12, ed. G. L. Messing, Shin-Ichi Hinamo & H. Haussen. The American Ceramic Society, Westerville, OH, 1990, p. 75.
6. Ishizawa, H., Sakurai, O., Mizutani, N. & Kato, M., Homogeneous Y<sub>2</sub>O<sub>3</sub>-stabilized ZrO<sub>2</sub> powder by spray pyrolysis method. *J. Am. Ceram. Soc.*, **65** (1986) 1399–406.
7. Kanno, Y. & Suzuki, T., Synthesis of fine spherical ZrO<sub>2</sub>-SiO<sub>2</sub> particles by ultrasonic spray pyrolysis. *J. Mater. Sci. Lett.*, **7** (1988) 386–92.
8. Lange, F. F., Powder processing science and technology for increased reliability. *J. Am. Ceram. Soc.*, **72** (1989) 3–15.
9. Rehspringer, J. L., Thesis, Strasbourg University, 1986.
10. Dubois, B., Cabannes, F., Ruffier, D. & Odier, P., Processing and sintering of 3Y-TZP prepared by a spray pyrolysis method. In *Proceedings of First Euro-Ceramics*, ed. G. de With, R. A. Terpstra & R. Metselaar. Elsevier Applied Science, pp. 1.431–1.435.